ELSEVIER

Journal of Alloys and Compounds 293–295 (1999) 546–551

Journal of ALLOYS AND COMPOUNDS

Hydriding properties of the heat-treated MgNi alloys with nanostructural designed multiphase

K. Yamamoto[a,*], S. Orimo[b,1], H. Fujii[b], Y. Kitano[c]

[a]*Hiroshima Prefectural Joint Research Center for Advanced Technology, Higashi-Hiroshima 739-0046, Japan*
[b]*Faculty of Integrated Arts and Sciences, Hiroshima University, Higashi-Hiroshima 739-8521, Japan*
[c]*Faculty of Integrated Science and Engineering, Shimane University, Matsue 690-8504, Japan*

Abstract

The structural and hydriding properties have been investigated for the heat-treated MgNi alloys with nanoscale structure which consists of the Mg_2Ni and $MgNi_2$ phases. The alloys were fabricated by mechanical alloying (MA) and heat treatment (HT), the so called MA/HT method. For the as-alloyed amorphous MgNi (a-MgNi) alloy, the maximum hydrogen content reaches 1.72 mass% at 473 K. The hydride, however, gradually decomposes into Mg_2NiH_4 and $MgNi_2$ phases during measurement of pressure–composition isotherm. In the case of nanoscaled crystalline Mg_2Ni (c-Mg_2Ni)+amorphous $MgNi_2$ (a-$MgNi_2$) multiphase alloy, the maximum hydrogen content reaches only 0.35 mass% at 473 K. No plateau-like behavior is observed in the desorption process. In the case of nanoscaled c-Mg_2Ni+crystalline $MgNi_2$ (c-$MgNi_2$) multiphase alloy, the maximum hydrogen content reaches 1.45 mass% at 473 K. A well-defined plateau region is observed of nearly 0.012 MPa at 473 K in the desorption process. Therefore, it is concluded that the hydriding properties of the nanoscaled MgNi multiphase alloy will be strongly affected by not only the structural properties of the matrix surrounding the c-Mg_2Ni grains precipitated but also by the accumulation/release of internal stress on the precipitation process.

Keywords: Hydrogen storage; Nanoscaled multiphase; Mechanical alloying; Heat treatment; Transmission electron microscopy

1. Introduction

A family of the Mg-based alloys is one of the attractive materials for hydrogen storage, because it is known to have a large amount of hydrogen capacity. Especially, the Mg–Ni alloys synthesized by mechanical alloying/grinding (MA/MG) have been extensively studied to produce the high-performance hydrogen storage materials having nanoscale structures [1–26]. In these works, it has been found that the amorphous MgNi (a-MgNi) alloy has notable hydriding properties [6,12,15,18,23–26]. From our systematic experimental works [21–26], it has been clarified that the a-MgNi alloy synthesized by MA of appropriate amounts of the Mg_2Ni intermetallic compound and elemental Ni has the following noticeable hydriding properties: The maximum hydrogen content is 2.2 mass% corresponding to a formula of $MgNiH_{1.9}$, and the dehydriding reaction occurs below 373 K in vacuum [23–25]. Furthermore, it has been clarified by the measurement of the electrochemical pressure–composition (p–c) isotherm that there is obviously the well-defined plateau region higher than 10^{-4} MPa at room temperature in the discharge process, even in the amorphous phase [26]. Therefore, the a-MgNi alloy has the possibility as a base material for fabrication of the new type of the hydrogen storage materials.

The a-MgNi alloy crystallizes into the multiphase with the Mg_2Ni and $MgNi_2$ phases by heat treatment (HT) [6,23]. On heating, two exothermic reactions are observed in the profile of the thermal analysis (see Fig. 1). The exothermic reactions around 603 K and 683 K correspond to the crystallization into the Mg_2Ni and $MgNi_2$ phases, respectively. Therefore, it would be possible to design various Mg–Ni alloys having nanoscale structures, which are mainly composed of the Mg_2Ni and $MgNi_2$ phases, by

*Corresponding author. Present address: Technical Research Center, Mazda Motor Corporation, Hiroshima 730-8670, Japan. Tel.: +81-82-252-5012; fax: +81-82-252-5342.

E-mail address: yamamoto.ken@lab.mazda.co.jp (K. Yamamoto)

[1]Present address: Max-Plank-Institut für Metallforschung, Institut für Physik, Heisenbergstrasse 1, 70569 Stuttgart, Germany.

0925-8388/99/$ – see front matter
PII: S0925-8388(99)00409-0

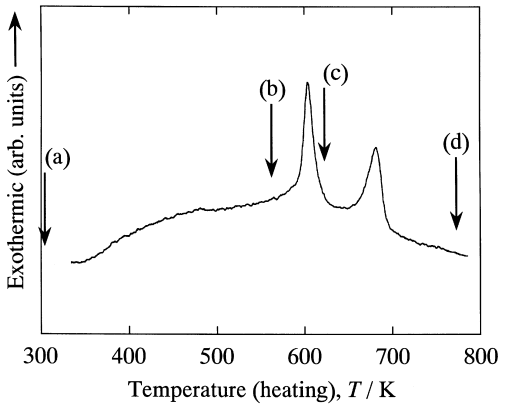

Fig. 1. DTA profile of the a-MgNi alloy obtained in this work. The DTA was carried out under a heating condition of 5 K min^{-1} up to 773 K in a purified argon gas flow of 50 cm^3 min^{-1}. The amount of the sample used for the DTA was nearly 40 mg. The temperatures of the heat treatments are pointed by the arrows, (a) as-alloyed, (b) 563 K, (c) 623 K and (d) 773 K.

suitable conditions of the HT. It is of interest to know the hydriding properties of the alloys with nanostructural multiphase from the viewpoint of the development of new Mg-based alloys for hydrogen storage. The purpose of this work is to clarify the relationship between structural and hydriding properties on the heat-treated MgNi alloy with nanoscale structures.

2. Experimental details

2.1. Sample preparation

The a-MgNi alloy was prepared as follows: A mixture of powders of Mg_2Ni (nearly 300 μm) and Ni (2–3 μm) was put into a steel vial together with 215 steel balls of 7 mm in diameter. Total amount of the powder mixture was 10 g, and the vial is equipped with a quick-released connecting valve for evacuation or introduction of gases. After introduction of the argon gas to a pressure of 0.2 MPa, the powder mixture was mechanically alloyed for 288 ks using a planetary ball mill apparatus (Fritsch P5) with a rotating speed of 200 rpm. The a-MgNi alloy obtained was fine powder of several micron meters in diameter. Therefore, the a-MgNi alloy obtained was carefully handled in an argon gas grove box to avoid oxidation.

The MgNi alloys with nanostructural multiphase were prepared by HT at suitable temperatures using the obtained a-MgNi alloy as a base material. The conditions of the HTs were determined from the result of the differential thermal analysis (DTA) for the a-MgNi alloy obtained. The DTA profile is shown in Fig. 1. Two exothermic peaks are observed around 600 K and 680 K in the profile, as firstly reported by Yang et al. [6], which correspond to the crystallization into the Mg_2Ni and $MgNi_2$ phases, respectively. The HTs of the alloys were carried out by heating up to (b) 563 K, (c) 623 K and (d) 773 K at a rate of 5 K min^{-1}, and by keeping these temperatures for 1 min.

2.2. Sample characterization

The structural properties of the samples were examined by the X-ray diffraction (XRD) with Cu–Kα radiation (Mac Science MXP3) and transmission electron microscopy (TEM) operated at 400 kV (JEOL JEM-4000EX). TEM specimens were prepared using the focused ion beam thinning technique with 30 kV Ga^+ ion (Hitachi FB-2000H). Details about the preparation of TEM specimens were described elsewhere [20,21,27,28].

The hydriding properties of the samples at 473 K were investigated using Sieverts-type apparatus. Prior to measuring the hydriding properties, the samples were heat-treated in the apparatus under the above condition in vacuum to prevent oxidation of the samples. After HT, the *p–c* isotherms in the desorption processes were measured under hydrogen gas pressures of 3–0.005 MPa at 473 K. Each data point was taken after 14.4–21.6 ks corresponding to the time which it requires to reach equilibrium.

3. Results

3.1. TEM observations

Typical examples of the TEM images of the heat-treated MgNi alloys are shown in Fig. 2. The selected area electron diffraction (SAED) pattern for the powder particle of each alloy is presented in Fig. 3. As seen in Fig. 2(a), the TEM image of the as-alloyed a-MgNi alloy shows gray and homogeneous, but sometimes shows a weak contrast suggesting an existence of Mg_2Ni or Ni nanocrystals whose diameters are in the range of 10–30 nm. The corresponding SAED pattern, Fig. 3(a), consists of halo rings. Since it is very rare for the diffraction spots to be observed, it could be concluded that an almost single phase of the a-MgNi alloy was formed by MA for 288 ks. For the alloy heat-treated at 563 K, the TEM image, Fig. 2(b), as well as SAED pattern, Fig. 3(b), show no prominent difference from the as-alloyed a-MgNi alloy except for a small increase in the number of nanocrystals. These nanocrystals would be precipitates which would appear at the first step of the crystallization process during HT at 563 K as a precursor of crystallization.

The nanostructures of the alloys heat-treated at 623 and 773 K were drastically changed. For the alloy heat-treated at 623 K, as seen in Fig. 2(c), the precipitates with 30–100 nm in diameter appear. In the corresponding SAED pattern, Fig. 3(c), the Debye–Scherrer rings of the Mg_2Ni phase are observed in addition to halo rings. This indicates that the precipitates discovered by TEM are the crystalline Mg_2Ni (c-Mg_2Ni), and that the gray matrix surrounding

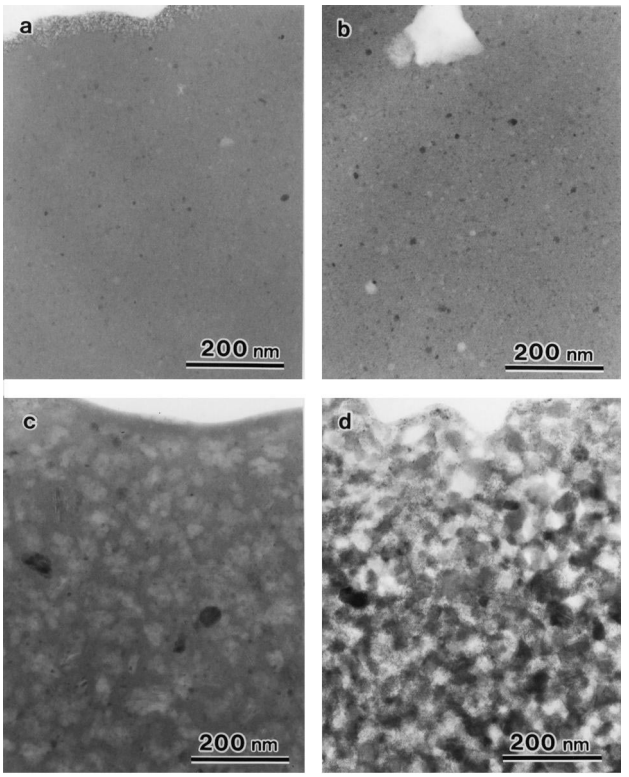

Fig. 2. Typical examples of the TEM images of the MgNi alloys which were (a) as-alloyed, and were heat-treated at (b) 563 K, (c) 623 K and (d) 773 K.

the precipitates is amorphous. Here, the amorphous would have a composition approximately equal to that of $MgNi_2$. Therefore, it can be concluded that the nanoscaled multiphase alloy which consists of the c-Mg_2Ni and amorphous $MgNi_2$ (a-$MgNi_2$) is synthesized by HT at 623 K.

In the case of the alloy heat-treated at 773 K, the whole of the alloy crystallizes into the nanocrystals of 30–100 nm in diameter. The TEM image of the alloy is presented in Fig. 2(d). The amorphous-like region is no longer observed in the image. The corresponding SAED pattern, Fig. 3(d), consists only of Debye–Scherrer rings of two phases, Mg_2Ni and $MgNi_2$, and no halo rings are observed. It is clear that the a-$MgNi_2$ phase having been formed at 623 K crystallizes into the nanocrystalline $MgNi_2$ (c-$MgNi_2$) at 773 K. Therefore, it can be concluded that the nanoscaled multiphase alloy which consists of two phases, c-Mg_2Ni and c-$MgNi_2$, is also synthesized by HT at 773 K. In the following sessions, we describe such nanoscaled multiphase alloys as c-Mg_2Ni+a-$MgNi_2$ and c-Mg_2Ni+c-$MgNi_2$, respectively.

3.2. Hydriding properties

On the basis of the results of TEM observations, the hydriding properties of the following three alloys were studied: (a) the as-alloyed a-MgNi, (c) nanoscaled c-Mg_2Ni+a-$MgNi_2$ multiphase and (d) nanoscaled c-Mg_2Ni+c-$MgNi_2$ multiphase alloys.

Fig. 4 shows the p–c isotherms of the alloys in the desorption process at 473 K under hydrogen pressures of 3–0.005 MPa. All the alloys easily reacted with the hydrogen from the early stage at this temperature under hydrogen pressure around 3 MPa. In the case of (a) the as-alloyed a-MgNi alloy, the maximum hydrogen content reaches 1.72 mass%, corresponding to nearly 80% of the maximum hydrogen content at room temperature [23–25]. Nearly 80% of the absorbed hydrogen atoms remain in the alloy even under 0.005 MPa. From the results of XRD analyses, however, it was found that the a-MgNi hydride gradually decomposed into the Mg_2NiH_4 and $MgNi_2$ phases during measurement of the p–c isotherm at 473 K. Here, it is to be noted that the hydrogen content curvilinearly decreases from 1 MPa to 0.1 MPa, reminiscent of a plateau-like behavior. In the case of (c) the nanoscaled c-Mg_2Ni+a-$MgNi_2$ multiphase alloy, the maximum hydrogen content is only 0.35 mass%. No decomposition of the alloy occurred in this case. The hydrogen content little changes by hydrogen gas pressure, and no plateau-like behavior is observed in the desorption process. Almost all of the absorbed hydrogen atoms remain in the alloy even under 0.005 MPa. In the case of (d) the nanoscaled c-Mg_2Ni+c-$MgNi_2$ multiphase alloy, the maximum hydrogen content reaches 1.45 mass%. No decomposition of the alloy also occurred in this case. It is noted that a well-defined plateau region is observed near 0.012 MPa in the desorption process, and nearly 80% of the absorbed hydrogen atoms is desorbed at this region. The value of this plateau pressure is slightly lower than that of the presumed plateau pressure of the bulky Mg_2Ni alloy, if the bulky Mg_2Ni alloy could desorb the hydrogen at 473 K (nearly 0.02 MPa, see the extrapolated line of Mg_2NiH_4 in Fig. 5).

4. Discussion

From the above experimental results, it is clear that the hydrogen properties of the MgNi alloys with nanoscaled multiphase are drastically affected by the structural properties of the alloys. This fact indicates that it is possible to design the various alloys which consist of plural nanoscaled phases, and in addition to fabricate the alloys which have notable hydriding properties by the MA/HT method.

The a-MgNi hydride gradually decomposed into Mg_2NiH_4 and $MgNi_2$ phases during the measurement of the p–c isotherm at 473 K. Orimo et al. [26] have reported that there is obviously the plateau pressure higher than 10^{-4} MPa at room temperature in the discharge process as a result of the electrochemical p–c isotherm measurement. Fig. 5 shows the van't Hoff plots of the typical hydrides

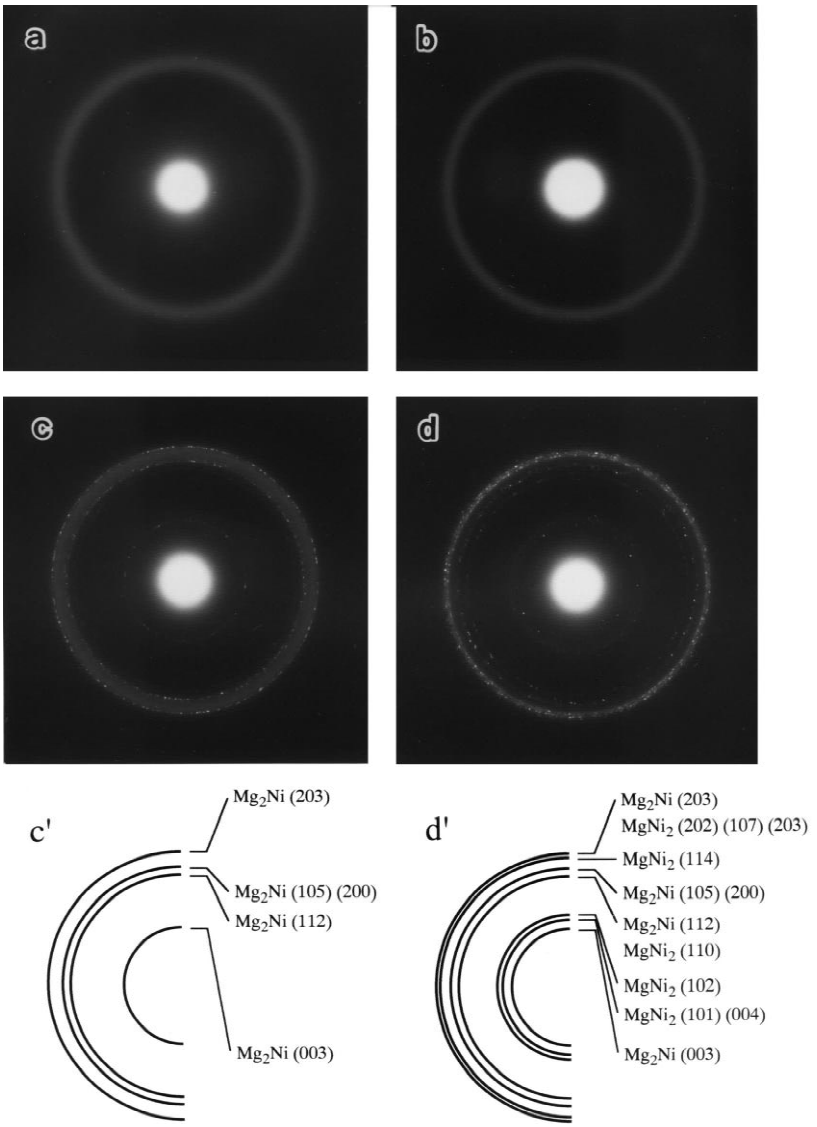

Fig. 3. SAED patterns from the powder particle of the MgNi alloys, each of which corresponds to that of Fig. 2. The diameter of the aperture used for the SAED patterns is about 500 nm.

and the a-MgNi hydride. Assuming that the formation entropies of the hydrides (ΔS) are approximately constant as is the case in the typical hydride (nearly -130 J K^{-1} molH_2^{-1}), the plot of the a-MgNi is deduced like a dashed line in this figure. If the a-MgNi hydride desorbs the hydrogen at 473 K without decomposition, the plateau region would appear between 0.1 and 1 MPa. Therefore, it is assumed that the curvilinear p–c isotherm between 1 MPa and 0.1 MPa which is shown in Fig. 4(a) contains the contribution from the plateau region of the a-MgNi hydride at 473 K, and that the dehydriding reaction is suppressed with progress of the decomposition of the a-MgNi hydride.

For the nanoscaled MgNi multiphase alloys, like the c-Mg_2Ni+a-$MgNi_2$ or c-Mg_2Ni+c-$MgNi_2$ multiphase, the maximum hydrogen content $H_{c\ max}$ (mass%) should be estimated from the following simple relation, if $H_{c\ max}$ of the alloys are given by the summation of those of the phases which constitute the alloys,

$$H_{c\ max} = h_{c1\ max} m_{f1} + h_{c2\ max} m_{f2} \quad (1)$$

where, $h_{c1\ max}$ and m_{f1} are the maximum hydrogen content (mass%) and the mass fraction of the phase 1 which constitute the nanoscaled multiphase alloys, respectively. In the case of the nanoscaled c-Mg_2Ni+a-$MgNi_2$ multiphase alloy, $H_{c\ max}$ is estimated to be 1.95 mass% using the values of the c-Mg_2Ni ($h_{c1\ max}=3.6$ and $m_{f1}=0.431$) and a-$MgNi_2$ ($h_{c2\ max}\sim0.7$ [29] and $m_{f2}=0.569$) phases, and the plateau region will be expected to appear at nearly 0.02 MPa at 473 K in the desorption process. Experimen-

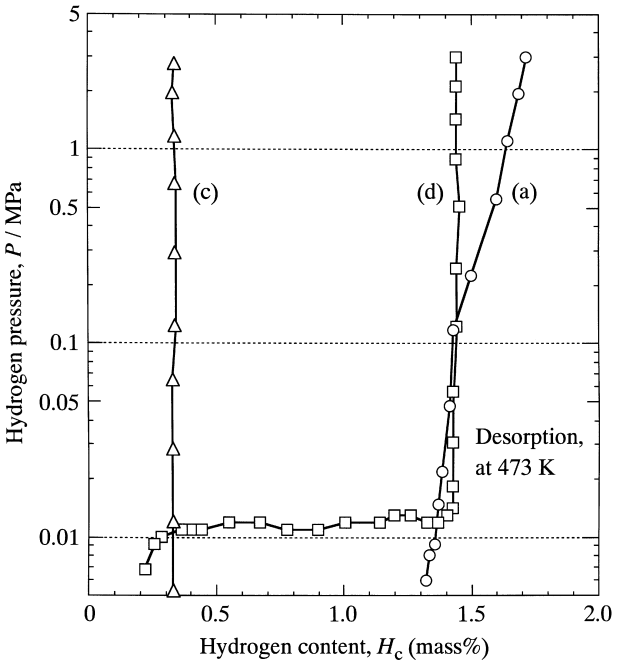

Fig. 4. p–c Isotherms in the desorption processes of the (a) as-alloyed a-MgNi, (c) nanoscaled c-Mg_2Ni+a-$MgNi_2$ multiphase and (d) nanoscaled c-Mg_2Ni+c-$MgNi_2$ multiphase alloys at 473 K under hydrogen pressures of 3–0.005 MPa.

tally, however, the maximum hydrogen content was only 0.35 mass%, and no plateau-like behavior was observed in the desorption process. These discrepancies would result from the structural properties of the matrix, — the a-$MgNi_2$ phase —, which surrounds the c-Mg_2Ni grains precipitated by HT. On the precipitation process of the c-Mg_2Ni grains, the internal stress in the c-Mg_2Ni grains would be stored, since the grains are perfectly surrounded by the a-$MgNi_2$ matrix, and the volume of the precipitated c-Mg_2Ni grains would be larger than that of the amorphous state. At the hydrogenation process in this case, the hydrogen atoms would diffuse from the surface of the alloy into the a-$MgNi_2$ matrix, and after then, start dissolving into the c-Mg_2Ni grains. At that time, the grains would undergo more higher internal stress. Therefore, it is assumed that the hydrogenation accompanied by volume expansion of the c-Mg_2Ni grains is suppressed because of the high internal stress. Consequently, the hydrogen atoms would dissolve into the c-Mg_2Ni grains with difficulty, and the hydrogen dissolved phase (α phase), $Mg_2NiH_{0.3}$, would be formed in addition to the a-$MgNi_2$ hydride.

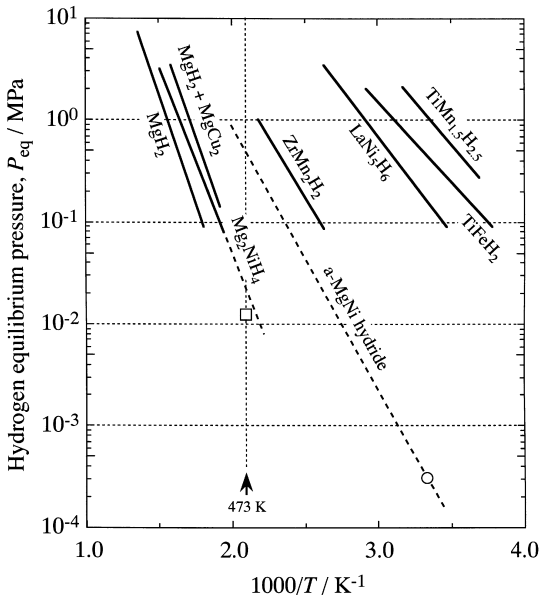

Fig. 5. Van't Hoff plots of the typical hydrides containing the a-MgNi hydride. The speculated line of the a-MgNi hydride and the extrapolated line of the bulky Mg_2NiH_4 are represented by the dashed lines. The open circle around 0.0003 MPa for the a-MgNi hydride indicates the observed point by the electrochemical p–c isotherm measurements [26]. The open square around 0.012 MPa indicates the observed point in this work for the nanoscaled c-Mg_2Ni+c-$MgNi_2$ multiphase alloys at 473 K.

In the case of the nanoscaled c-Mg_2Ni+c-$MgNi_2$ multiphase alloy, $H_{c\ max}$ is estimated to be 1.55 mass% by the values of c-Mg_2Ni ($h_{c1\ max}=3.6$ and $m_{f1}=0.431$) and c-$MgNi_2$ ($h_{c2\ max}=0$ and $m_{f2}=0.569$) phases, and the plateau region will be expected to appear nearly at 0.02 MPa at 473 K in the desorption process. In fact, the maximum hydrogen content reached 1.45 mass%. This value agrees very closely with the estimated value mentioned above. In addition, a well-defined plateau region was observed near 0.01 MPa in the desorption process, experimentally. These good agreements would be attributed to the structural properties of the matrix, — the c-$MgNi_2$ phase —, which surrounds the c-Mg_2Ni grains precipitated by HT. On the precipitation process of the c-$MgNi_2$ grains, the internal stress of the c-Mg_2Ni grains precipitated in preference to c-$MgNi_2$ grains would be released by crystallization of the a-$MgNi_2$ phase into the c-$MgNi_2$ phase because of the smaller volume of the precipitated c-$MgNi_2$ grains than that of the a-$MgNi_2$ matrix. At the hydrogenation process in this case, the hydrogen atoms would diffuse directly into the c-Mg_2Ni grains or along the grain boundaries of the c-$MgNi_2$ grains. Consequently, the hydrogen atoms would readily dissolve into the c-Mg_2Ni grains without internal stress, and the hydride phase (β phase), Mg_2NiH_4, would be formed. Therefore, it seems that these type of the alloys follows the sum rule of Eq. (1). On the other hand, the value of the plateau pressure was a little low compared to that of the bulky Mg_2Ni alloy. This would be because the hydrides of the c-Mg_2Ni grains with nanoscale diameter will be more stable than that of the bulky Mg_2Ni alloy [8,9].

From the above experimental results, it is concluded that the hydriding properties of the nanoscaled MgNi multiphase alloy fabricated in this study will be strongly affected by not only the structural properties of the matrix surrounding the c-Mg_2Ni grains precipitated but also the accumulation/release of internal stress on the precipitation process.

5. Conclusion

In this work, the MgNi alloys with nanoscaled multiphase, which were fabricated using the combination method of MA and HT, were investigated to clarify the relationship between structural and hydriding properties in the nanostructures. From the experimental results, it is concluded that the hydriding properties of the nanoscaled MgNi multiphase alloy will be strongly affected by not only the structural properties of the matrix surrounding the c-Mg_2Ni grains precipitated but also the accumulation/release of internal stress on the precipitation process. The results obtained in this work suggest that the hydriding properties of the Mg-based alloys will be improved by the application of nanostructural designation using the MA/HT method.

Acknowledgements

This work was financially supported by Hiroshima Prefecture in Japan.

References

[1] M.Y. Song, E.I. Ivanov, B. Darriet, M. Pezat, P. Hagenmuller, Int. J. Hydrogen Energy 10 (1985) 169.
[2] E. Ivanov, I. Konstanchuk, A. Stepanov, V. Boldyrev, J. Less-Common Met. 131 (1987) 25.
[3] M.Y. Song, E. Ivanov, B. Darriet, M. Pezat, P. Hagenmuller, J. Less-Common Met. 131 (1987) 71.
[4] A. Stepanov, E. Ivanov, I. Konstanchuk, V. Boldyrev, J. Less-Common Met. 131 (1987) 89.
[5] K. Aoki, H. Aoyagi, A. Memezawa, T. Masumoto, J. Alloys Comp. 203 (1994) L7.
[6] Q.M. Yang, Y.Q. Lei, C.P. Chen, J. Wu, Q.D. Wang, G.L. Lu, L.S. Chen, Z. Phys. Chem. 183 (1994) 141.
[7] A.K. Singh, A.K. Singh, O.N. Srivastava, J. Alloys Comp. 227 (1995) 63.
[8] L. Zaluski, A. Zaluska, J.O. Ström-Olsen, J. Alloys Comp. 217 (1995) 245.
[9] L. Zaluski, A. Zaluska, P. Tessier, J.O. Ström-Olsen, R. Schulz, J. Alloys Comp. 217 (1995) 295.
[10] J. Huot, E. Akiba, T. Takada, J. Alloys Comp. 231 (1995) 815.
[11] M.Y. Song, Int. J. Hydrogen Energy 20 (1995) 221.
[12] D.L. Sun, Y.Q. Lei, W.H. Liu, J.J. Jiang, J. Wu, Q.D. Wang, J. Alloys Comp. 231 (1995) 621.
[13] H. Aoyagi, K. Aoki, T. Masumoto, J. Alloys Comp. 231 (1995) 804.
[14] T. Kohno, S. Tsuruta, M. Kanda, J. Electrochem. Soc. 143 (1996) L198.
[15] C. Iwakura, S. Nohara, H. Inoue, Y. Fukumoto, Chem. Commun. 15 (1996) 1831.
[16] S. Orimo, H. Fujii, J. Alloys Comp. 232 (1996) L16.
[17] S. Orimo, H. Fujii, K. Ikeda, Y. Kitano, J. Jpn. Inst. Metals 60 (1996) 685, (in Japanese).
[18] W.H. Liu, H.Q. Wu, Y.Q. Lei, Q.D. Wang, J. Alloys Comp. 252 (1997) 234.
[19] S. Orimo, H. Fujii, K. Ikeda, Acta Mater. 45 (1997) 331.
[20] Y. Kitano, Y. Fujikawa, N. Shimizu, S. Orimo, H. Fujii, T. Kamino, T. Yaguchi, Intermetallics 5 (1997) 97.
[21] K. Yamamoto, Y. Fujikawa, K. Ikeda, S. Orimo, H. Fujii, Y. Kitano, J. Electron Microsc. 47 (1998) 461.
[22] S. Orimo, K. Ikeda, H. Fujii, K. Yamamoto, J. Alloys Comp. 260 (1997) 143.
[23] S. Orimo, K. Ikeda, H. Fujii, Y. Fujikawa, Y. Kitano, K. Yamamoto, Acta Mater. 45 (1997) 2271.
[24] S. Orimo, H. Fujii, K. Ikeda, Y. Fujikawa, Y. Kitano, J. Alloys and Comp. 253/254 (1997) 94.
[25] S. Orimo, H. Fujii, Intermetallics 6 (1998) 185.
[26] S. Orimo, K. Ikeda, H. Fujii, S. Saruki, T. Fukunaga, A. Züttel, L. Schlapbach, Acta Mater. (in press).
[27] Y. Kitano, Y. Fujikawa, H. Takeshita, T. Kamino, T. Yaguchi, H. Matsumoto, H. Koike, J. Electron Microsc. 44 (1995) 376.
[28] Y. Kitano, Y. Fujikawa, T. Kamino, T. Yaguchi, H. Saka, J. Electron Microsc. 44 (1995) 410.
[29] S. Orimo, H. Fujii, private communication.